2020 IEEE/RSJ International Conference on Intelligent Robots and Systems (IROS)
October 25-29, 2020, Las Vegas, NV, USA (Virtual)

Variable Pitch System for the Underwater Explorer Robot UX-1*

Ramon A. Suarez Fernandez[1] Davide Grande[2], Alfredo Martins[3], Luca Bascetta[2], Sergio Dominguez[1] and Claudio Rossi[1]

***Abstract*— This paper presents the results of the experimental tests performed to validate the functionality of a variable pitch system (VPS), designed for pitch attitude control of the novel underwater robotic vehicle explorer UX-1. The VPS is composed of a mass suspended from a central rod mounted across the hull. This mass is rotated around the transverse axis of the vehicle in order to perform a change in the inclination angle for navigation in vertical mine shafts. In this work, the equations of motion are first derived with a quaternion attitude representation, and are then extended to include the dynamics of the VPS. The performance of the VPS is demonstrated in real underwater experimental tests that validate the pitch angle control independently, and coupled with the heave motion control system.**

I. Introduction

Underwater vehicles are flourishing, performing key roles in a number of scientific and commercial endeavors. Recently, the focus of several research lines has been aimed at developing solutions for advanced underwater vehicles, designed to operate in complex environments, such as under ice shelves [1], where access is virtually impossible by any other means. Most scientific applications in these challenging environments include mapping, survey, and inspection tasks [2] [3]. However, a unique cutting-edge application for underwater robotics is the exploration of flooded underground mines.

In an effort to locate a sustainable supply of raw materials from European sources, interest has been directed towards determining the feasibility of re-opening some of the nearly 30,000 inactive or abandoned underground mines across Europe, which may contain a considerable amount of raw material reserves considered critical. Hence, the UNEXMIN project has developed a novel underwater robotic platform system named UX-1, to explore flooded mines and acquire geo-scientific and topological data. The development of UX-1 will open new exploration scenarios, so that strategic decisions on dewatering and re-starting exploitation of Europe's abandoned mines can be supported by real data, which cannot be gathered in any other way. This challenging operational environment intended as the workspace for the UX-1 platform, and the novelty of the vehicle's mechanical design, require the development of innovative actuation components that comply with the required objectives of the foreseen exploration missions.

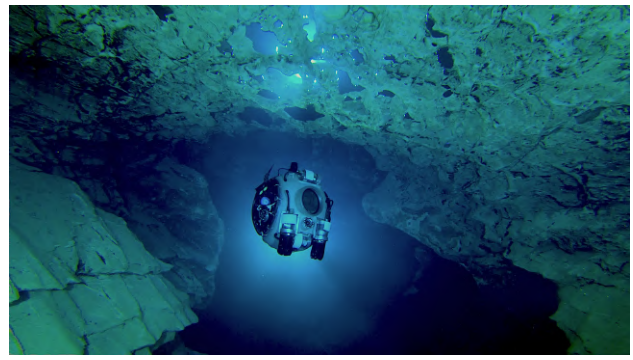

Fig. 1. UX-1 underwater vehicle during field tests in the Molar Janos cave system in Budapest, Hungary.

According to the design requirements specified by the end-users of the UX-1 platform [4], the underwater vehicle must be capable of shifting the inclination angle (*pitch* motion), in order to navigate facing the direction of movement in vertical or slanted shafts. This requirement arises from the placement of the majority of the external sensors in the front of the UX-1 vehicle, i.e., MultiBeam SONAR, cameras, laser scanners, etc. This work presents the validation and experimental testing of a custom built Variable Pitch System (VPS) motion component which was designed to actively change the center of gravity (CG) of the UX-1 underwater vehicle by rotating a mass, suspended below the center of buoyancy (CB), about the transverse axis of the vehicle. This shifting of a mass w.r.t. the CG of the vehicle generates a torque which in turn rotates the UX-1 vehicle to a desired pitch angle, passively stabilizing the system.

Several works in underwater robotics can be found in the literature that have exploited the possibility of shifting internal masses to achieve efficient attitude control, more commonly known as a mass shifting mechanism (MSM). Examples of underwater vehicles using linear MSMs are the Seaglider [5] and the Slocum [6]. Further details about the MSM and the related control strategies can be found in [7] and [8]. This approach turns out to be suitable whenever the

*This work was supported by the UNEXMIN project with funding from the European Union's Horizon 2020 research and innovation programme under Grant Agreement No. 690008, and has been co-funded by the RoboCity2030-DIH-CM Madrid Robotics Digital Innovation Hub ("Robotica aplicada a la mejora de la calidad de vida de los ciudadanos. fase IV"; S2018/NMT-4331), funded by "Programas de Actividades I+D en la Comunidad de Madrid" and cofunded by Structural Funds of the EU.

[1]Ramon A. Suarez Fernandez, Sergio Dominguez and Claudio Rossi are with the Center for Automation and Robotics, Universidad Politécnica de Madrid, Madrid 28006, Spain. fernandez.suarez.ramon@gmail.com, {claudio.rossi, sergio.dominguez}@upm.es.

[2]Davide Grande and Luca Bascetta are with the Dipartimento di Elettronica, Informazione e Bioingegneria, Politecnico di Milano, Milan, Italy {davide1.grande, luca.bascetta}@polimi.it

[3]Alfredo Martins is with the INESC-TEC, Instituto Superior de Engenharia do Porto, Portugal aom@lsa.isep.ipp.pt

mission environment requires occasional attitude changes, rather than fast and repeated control inputs. For instance, this is the case of torpedo-shaped vehicles (i.e., [5], [6]) that need to keep a quasi-constant pitch angle to change depth.

Moreover, the mass shifting technique is particularly efficient, with respect to the traditional control method of using a set of fins, whenever the cruise speeds need to be maintained low. In fact, shifting the center of mass of the vehicle induces a change in the attitude in spite of the velocities experienced by the vehicle, whereas the actuation by means of the fins presents the additional constraint of relying on a minimum speed to be effective. Linear MSM are generally suitable for torpedo-shaped vehicles that can fit the length of the stroke. Therefore, due to the required mechanical design of the underwater vehicle used in this work, linear MSM designs cannot be efficiently allocated into a spherical compact underwater vehicle, such as the UX-1.

Robots with spherical morphology recently gained popularity and are being developed for various fields, such as surveillance using the GroundBot [9] [10], or even for planetary exploration, as reported for the Spherical Mobile Investigator for Planetary Surface (SMIPS) in [11]. The same strategy can be extended to underwater field applications. The Eyeball Remotely Operated Vehicle (ROV) [12], similar to the UX-1 platform, is aimed at inspecting underwater structures in hazardous environments. The Eyeball ROV uses a gimbal mechanism to displace an internal eccentric mass and consequently to perform a turning motion in-place, that in narrow environments helps reducing the risk of entanglements or collision with protruding objects. Nonetheless, the specific combination of operational speeds specified for the UX-1 (1.5 – 2 m/s), the hazardous operating environments and the requirement for energy efficiency, deem the various attitude control mechanisms found in the literature unsuitable for integration in the UX-1 underwater vehicle.

The work in this paper is presented as follows: Section II introduces the basic aspects of the mechanical design and integration of the VPS for the UX-1 vehicle, whilst in Section III the complete dynamic model of the underwater vehicle system is derived, with the inclusion of the dynamics generated by the VPS motion component. Afterwards, Section IV presents the results achieved with the performed experimental validation tests. Lastly, conclusions and future works are detailed in Section V.

II. VPS Mechanical Design

As it can be seen in [13] and [14], the design of the primary propulsion system for the UX-1 platform integrated the actuators (i.e., 8 BlueRobotics[1] T200 thrusters) in a cross-manifold configuration, so as to avoid any possibility of entanglement, and increased fault tolerance introducing overactuation. Nonetheless, this cross-manifold configuration of the actuators only achieved 5 degree-of-freedom (DOF) motions, namely, *Surge*, *Sway*, *Heave*, *Roll*, and *Yaw*. In order to obtain the full 6 DOF motion of the underwater vehicle, a VPS motion component, based on the principle of counterweights rotating around an axis, has been designed and integrated. The complete mechanical design of the VPS, as well as initial computer simulations, can be found in [17].

[1]www.bluerobotics.com

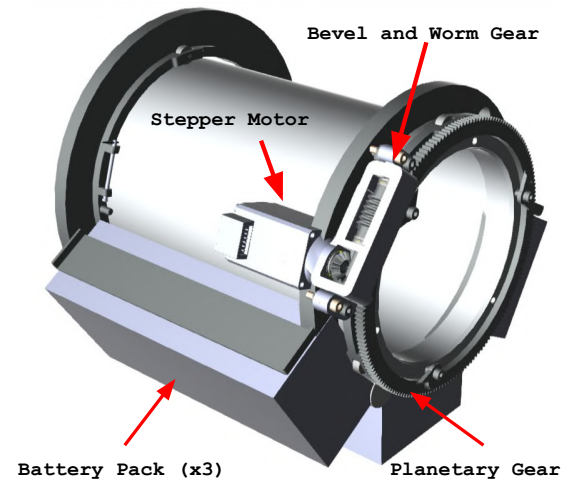

Fig. 2. 3D CAD model of the VPS design with the planetary gear, stepper motor, and bevel and worm gear set-up.

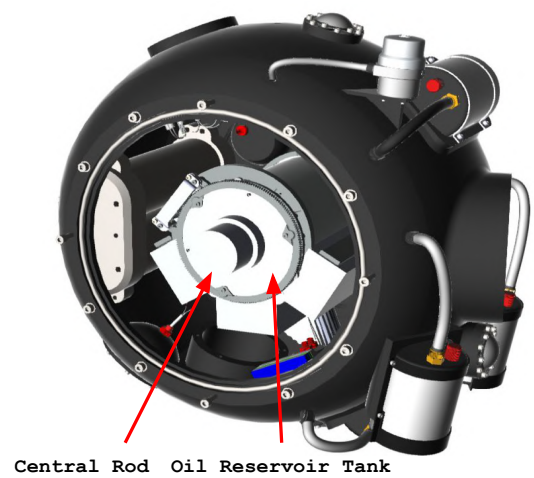

Fig. 3. CAD model of the Variable Pitch System installation on the UX-1 Robot.

The VPS motion component was designed to maximize the operation time during dives, by using a low power consumption implementation. As it can be seen in Fig. 2, the VPS consists of a stepper motor with a bevel and worm gear set-up, which rotates the battery pack (three eccentrically placed 6S 16000 mAh LiPo batteries) around the central rod (CR) oil reservoir tank (see Fig. 3), using a planetary gear fixed to the CR [16]. Fig. 3 shows the 3D CAD model of the UX-1 vehicle with the final design of the VPS integrated into the hull.

III. System Dynamic Model

The nonlinear dynamic model of the UX-1 underwater vehicle has been previously studied and derived in var-

ious works found in the literature. In [13], a model of a spherical underwater vehicle was presented, which was derived based on the initial design specifications of the UX-1 vehicle. Moreover, [14] presents experimental tests which were performed to identify several model parameters of the real underwater platform, and to obtain the high-fidelity 6 DOF equations of motion of the UX-1 underwater vehicle. This dynamic model was subsequently used for model-based control system design and validation. In this work, the previously derived 6 DOF dynamic model is extended, by integrating the reaction forces and torques generated by the VPS motion component into the equations of motion of the system.

A. 6 DOF Equations of Motion

In this work, two reference frames are assumed, $\{i\}$, and $\{b\}$, which are represented in the world coordinate system. Reference frame $\{i\}$ denotes an inertial North-East-Down (NED) coordinate system with orthogonal basis $\{x_i, y_i, z_i\}$ and origin o_i, whilst $\{b\}$ denotes a body-fixed reference frame (located at the geometrical center of the vehicle) with orthogonal basis $\{x_b, y_b, z_b\}$ and origin o_b. Using the Society of Naval Architects and Marine Engineers (SNAME) nomenclature in [19], the equations of motion are derived using the following notation in vectorial form [18],

$$\boldsymbol{\eta} = \begin{bmatrix} \boldsymbol{P} \\ \boldsymbol{q} \end{bmatrix} = [x, y, z, q_0, q_1, q_2, q_3]^\top \tag{1}$$

$$\boldsymbol{\nu} = \begin{bmatrix} \boldsymbol{v} \\ \boldsymbol{\omega} \end{bmatrix} = [u, v, w, p, q, r]^\top \tag{2}$$

$$\boldsymbol{\tau} = \begin{bmatrix} \boldsymbol{f} \\ \boldsymbol{m} \end{bmatrix} = [X, Y, Z, K, M, N]^\top \tag{3}$$

where $\boldsymbol{\eta} \in \mathbb{R}^7$ denotes the position ($\boldsymbol{P} \in \mathbb{R}^3$) and orientation ($\boldsymbol{q} \in \mathbb{R}^4$) vectors, $\boldsymbol{\nu} \in \mathbb{R}^6$ denotes the linear ($\boldsymbol{v} \in \mathbb{R}^3$) and angular ($\boldsymbol{\omega} \in \mathbb{R}^3$) velocity vectors in $\{b\}$, and in (3), $\boldsymbol{\tau} \in \mathbb{R}^6$ is used to describe the forces ($\boldsymbol{f} \in \mathbb{R}^3$) and moments ($\boldsymbol{m} \in \mathbb{R}^3$) acting on the vehicle in $\{b\}$. The 6 DOF equations of motion are expressed with a quaternion attitude representation in the body-fixed reference frame $\{b\}$ as:

$$\dot{\boldsymbol{\eta}} = \boldsymbol{J}_q^\dagger(\boldsymbol{\eta})\boldsymbol{\nu} \tag{4}$$

$$\boldsymbol{M}\dot{\boldsymbol{\nu}} + \boldsymbol{C}(\boldsymbol{\nu})\boldsymbol{\nu} + \boldsymbol{D}(\boldsymbol{\nu})\boldsymbol{\nu} + \boldsymbol{g}(\boldsymbol{\eta}) = \boldsymbol{\tau} \tag{5}$$

with

$$\boldsymbol{M} = \boldsymbol{M}_{RB} + \boldsymbol{M}_A \tag{6}$$

$$\boldsymbol{C}(\boldsymbol{\nu}) = \boldsymbol{C}_{RB}(\nu) + \boldsymbol{C}_A(\nu) \tag{7}$$

$$\boldsymbol{D}(\boldsymbol{\nu}) = \boldsymbol{D} + \boldsymbol{D}_n(\boldsymbol{\nu}) \tag{8}$$

where (4) and (5) define the kinematic and dynamic models, respectively. In (4), $\boldsymbol{J}_q^\dagger(\boldsymbol{\eta})$ is the left Moore-Penrose pseudo-inverse of the non-quadratic transformation matrix $\boldsymbol{J}_q(\boldsymbol{\eta}) \in \mathbb{R}^{7\times 6}$, and $\boldsymbol{g}(\boldsymbol{\eta})$ is the vector of gravitational and buoyant forces. $\boldsymbol{M}$ is the system inertia matrix composed of the rigid-body inertia matrix $\boldsymbol{M}_{RB}$, and the hydrodynamic inertia matrix of added mass terms $\boldsymbol{M}_A$. The Coriolis-centripetal term matrix $\boldsymbol{C}(\boldsymbol{\nu})$, consists of the rigid-body $\boldsymbol{C}_{RB}(\nu)$, and hydrodynamic $\boldsymbol{C}_A(\nu)$ matrices. Lastly, the total hydrodynamic damping matrix $\boldsymbol{D}(\boldsymbol{\nu})$ is the sum of the linear term $\boldsymbol{D}$, and the nonlinear term $\boldsymbol{D}_n(\boldsymbol{\nu})$. The UX-1 vehicle model matrices (i.e., $\boldsymbol{M}$, $\boldsymbol{C}(\boldsymbol{\nu})$, $\boldsymbol{D}(\boldsymbol{\nu})$, $\boldsymbol{g}(\boldsymbol{\eta})$) definitions and properties can be found in [14].

B. VPS Model Integration

The dynamic model of the UX-1 underwater vehicle can be obtained by extending the 6 DOF nonlinear equations of motion presented in (4) and (5). Nevertheless, in order to consider the full dynamic behavior of the UX-1 platform, the forces and torques generated by the VPS must be incorporated into the equations of motion. Consequently, the overall system will be considered as two independent bodies: the external hull and the internal VPS.

The VPS is modeled as a pendulum system rigidly attached to the external hull of the underwater vehicle by a planar hinge, which constrains the movement of the pendulum to 1 DOF (the rotation around the hinge). This results in an overall system with 7 DOF. All of the forces acting on the vehicle described so far (i.e., $\boldsymbol{g}(\eta)$ and $\boldsymbol{\tau}$), with the addition of the weight force of the hull, have been applied to the geometrical center of the vehicle; whereas, the gravity force of the VPS is applied to its center of mass. Moreover, the hinge is considered an ideal rigid joint where no losses due to friction take place.

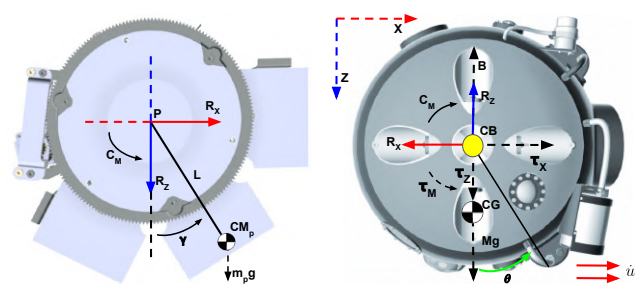

(a) (b)

Fig. 4. Diagram of the external forces and moments on: (a) the VPS; and (b) the UX-1.
https://www.overleaf.com/project/5efdc64e186edf0001a7dee2
https://www.overleaf.com/project/5efdc64e186edf0001a7dee2

The forces and torques are derived by analyzing the forces acting upon the VPS as a stand alone body. Based on the free-body diagram shown in Fig. 4(a), the vertical and horizontal components of the pendulum mass center are $z + L\cos(\gamma)$ and $x + L\sin(\gamma)$, respectively. Newton's second law gives

$$m_p \frac{d^2}{dt^2}(x + L\sin(\gamma)) = R_X \tag{9}$$

$$m_p \frac{d^2}{dt^2}(z + L\cos(\gamma)) = R_Z + m_p g. \tag{10}$$

where R_X and R_Z are the horizontal and vertical components of the reaction forces at the pivot point (P). Evaluating

the derivatives in (9) and (10), results in:

$$m_p\dot{u} + m_p\ddot{\gamma}L\cos(\gamma) - m_p\dot{\gamma}^2 L\sin(\gamma) = R_X \quad (11)$$
$$m_p\dot{w} - m_p\ddot{\gamma}L\sin(\gamma) - m_p\dot{\gamma}^2 L\cos(\gamma) - m_p g = R_Z. \quad (12)$$

Similarly, the expression for the moment about the pendulum pivot point is given by:

$$C_M = m_p\ddot{\gamma}L^2 + m_p\dot{u}L\cos(\gamma) + m_p gL\sin(\gamma) \quad (13)$$

where the mass of the pendulum is denoted by m_p, which considers only the weight of the three eccentrically placed batteries lumped into the center of mass of the pendulum. g is the force from gravity. The length of the pendulum arm is denoted by L, and the pendulum angle γ is represented as positive counterclockwise around the transverse axis of the UX-1 vehicle, namely y_b. Since the VPS is constrained to a planar movement around the transverse axis of the vehicle, and the roll is inherently stable by design, the pendulum reaction forces and moments will only affect the longitudinal dynamics of the underwater vehicle. Furthermore, they will be assumed as external forces ($\boldsymbol{\tau_{ext}}$) to be added to the previously computed 6 DOF equations of motion forces and moments vector $\boldsymbol{\tau}$, which results in $\boldsymbol{\tau_{ext}} = [-R_X, 0, -R_Z, 0, -C_M, 0]^\top$.

The expanded 7 DOF model of the underwater vehicle is defined by combining the pendulum reaction equations in (11), (12), and (13), with the equations of motion of the underwater vehicle in (4) and (5).

IV. Results and Discussion

In this section, the experimental results will be presented and analyzed. The verification and validation of the VPS motion component for pitch control was carried out with several experimental tests, during the field trials performed at the Ecton copper mine in the United Kingdom.

A. Experimental Set-up.

The initial testing of the VPS mechanism focused as a proof-of-concept to validate the design of the actuator, as such, the control input for the VPS motion component was chosen as incremental changes in pendulum angle (γ), for which a basic proportional control law ($\gamma = K_p e_\gamma$) was integrated in the motion control system software architecture, running at 20 Hz. Where e_γ is the error between the current pitch angle, hereby reported as θ, and the setpoint reference. The results obtained with this control law will be used as a baseline for future implementations of more advanced control algorithms.

The hardware interface for the VPS was developed using CAN bus communications. Moreover, to maintain scalability with the previous components of the software architecture, the open source Robot Operating System (ROS) middleware framework was used to handle intercommunication between processes. All nodes have been implemented in Python or C++ in the Com Express Type 6 on-board main PC, running the GNU/Linux operating system Ubuntu 16.04 LTS.

B. Pitch Motion Tests

The preliminary experimental tests were carried out to evaluate the response of the VPS motion component for a pitch angle regulation task. Three pitch configurations were considered crucial for navigation in mine tunnels, i.e., nose-front ($\theta \approx 0$ rad), nose-up ($\theta \approx \frac{\pi}{2}$ rad), and nose-down ($\theta \approx -\frac{\pi}{2}$ rad).

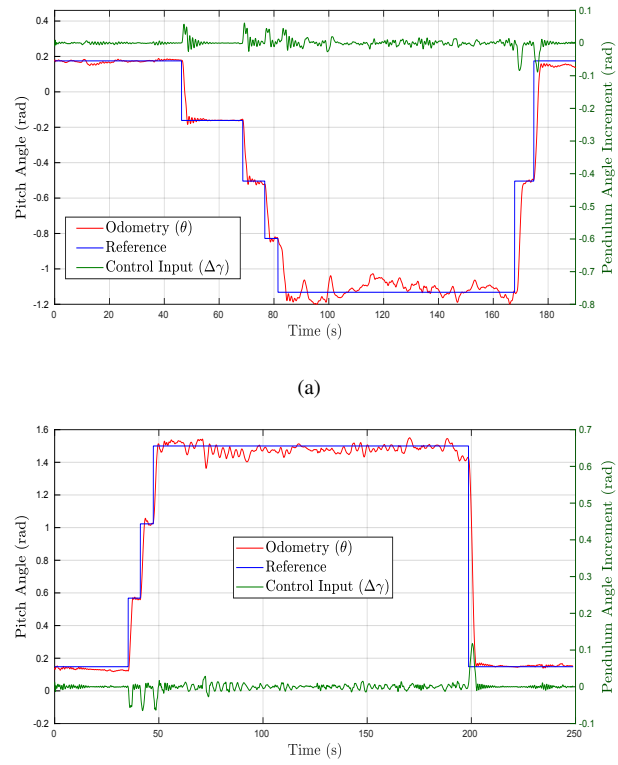

Fig. 5. Experimental tests performed with the VPS to control the pitch angle of the UX-1 vehicle. (a) Nose down and (b) Nose up motions.

As it can be seen in Fig. 5(a), starting from a nose-front pitch setpoint of $\theta = 0.175$ rad, a series of negative pitch reference commands were sent, which relate to a nose-down motion of the UX-1 underwater vehicle, until a pitch of approximately $\theta = -1.132$ rad was reached. At this pitch angle, the underwater vehicle was kept nearly parallel to the shaft of the tunnel, before returning the reference to a nose-front configuration at a pitch angle of $\theta = 0.175$ rad. Once the nose-down pitch motion of the underwater vehicle was tested, the nose-up (counterclockwise rotation) configuration test was performed. The response of the VPS for this test is presented in Fig. 5(b). Similar to the previous test, step reference pitch angles were applied until an angle of $\theta = 1.50$ rad was obtained, maintaining this nose-up for a span of 150 s. Afterwards, the configuration was changed directly from nose-up to nose-front in order to test the response of the VPS for a larger step reference command.

Table I shows the time response analysis for the pitch motion tests presented in Fig. 5. The chosen time response

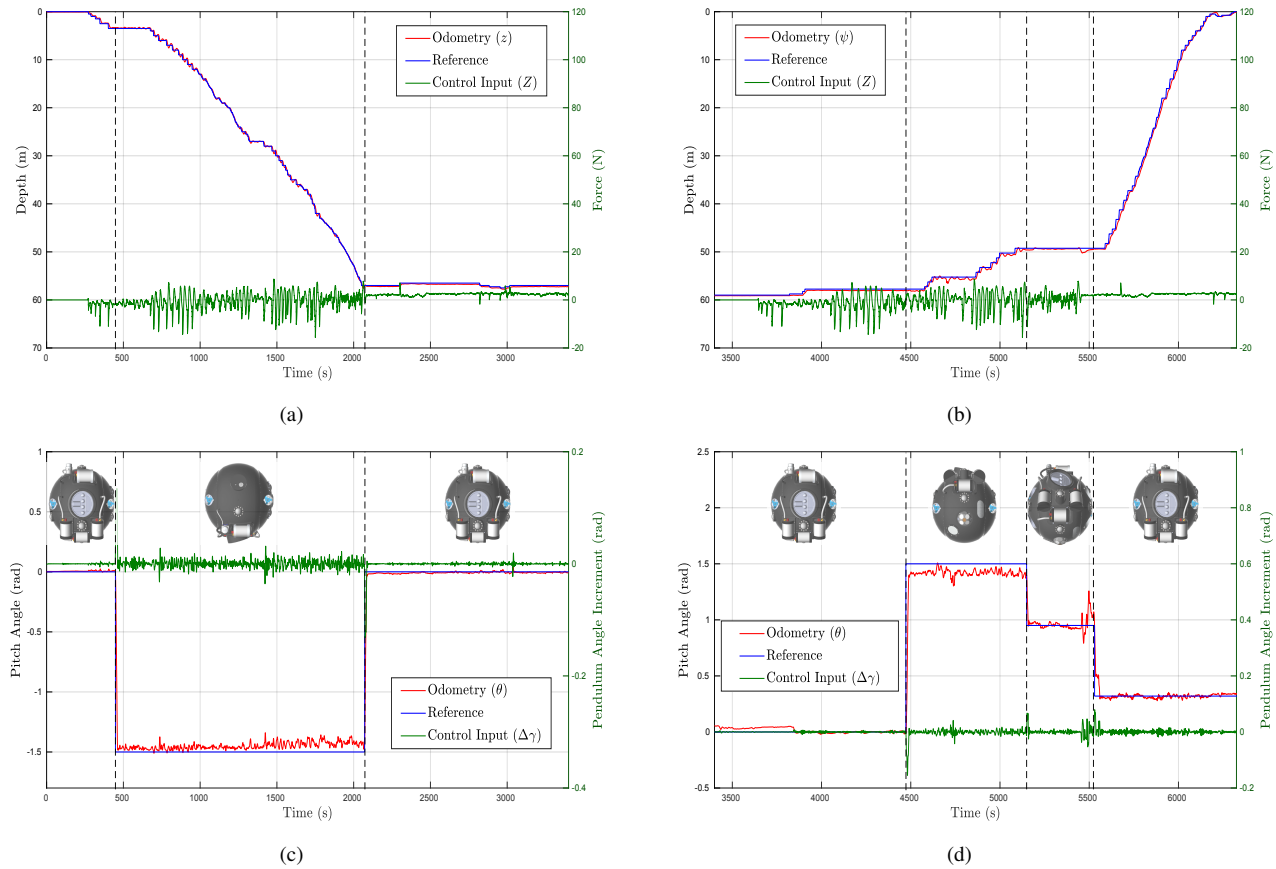

Fig. 6. Experimental test performed with coupled motions. The dashed lines represent the instants where a configuration change was commanded for the pitch angle and the vehicle configurations associated with the the commanded pitch angles are shown on top of the signals for clarity. (a)–(b) Response of the depth motion control system of the UX-1 vehicle during experiment. (c)–(d) Response of the pitch angle using the VPS during the coupled experiment.

metrics were: Overshoot percentage ($OS\%$), Rise time (T_r), Fall time (T_f), Settling time (T_s) and Root-Mean-Square Error (RMSE). The results validate the functionality and performance of the VPS for the overall requirements, established as achieving an $OS\%$ of less than 10% and a RMSE of 0.1 rad. The implemented proportional control law achieved a RMSE of 0.092 rad and 0.109 rad for the nose-down and nose-up motions, respectively. The transient response of the system can be considered to have slow dynamics, which is a consequence of limitations in space/power of the mechanical components. Nevertheless, since the UX-1 platform is intended to perform at low speeds, these values are not considered crucial. Moreover, it was noticed that at the critical pitch reference angles for complete nose-up or nose-down configurations, the response of the system became unstable and oscillating, which can be appreciated by the control input plots in Fig. 5. This behavior had no noticeable effect on the performance of the VPS and was only shown at these configurations because of an unbalanced weight distribution unnoticed prior to the descent, which affected the buoyancy of the underwater platform.

C. Coupled Motion Tests

The main motivation behind the design and integration of the VPS is to have the ability to navigate with the front of the UX-1 vehicle facing the desired direction of travel during exploration missions. Hence, once the pitch angle control was validated, a coupled motion experiment was performed. For this test, the pitch and heave motion controllers were active simultaneously throughout the dive. The depth controller is based on Feedback Linearization, where the design, testing and experimental validation can be found in [15] [14]. Fig. 6 shows the results of the exploration mission with insets of the pitch configuration at different stages of the dive, as well as the force output from the depth controller and the control input for the VPS from the proportional controller implemented.

The UX-1 platform was submerged to 60 m using the depth controller. During the descent (see Fig. 6(a)), the pitch

TABLE I
TIME RESPONSE ANALYSIS FOR VPS PITCH CONTROL TESTS.

	Pitch Motion		
Metrics	Nose Down	Nose Up	Units
T_r	—-	7.125	[s]
T_f	8.526	—-	[s]
T_s	8.045	13.831	[s]
OS%	9.330	5.014	[%]
RMSE	0.092	0.109	[rad]

angle was set to $\theta = -1.5$ rad to navigate nose-down along the shaft from $t \approx 250$ s to $t \approx 2000$ s, shown in Fig. 6(c).

Once the desired depth was reached, the pitch angle was set to a nose-front configuration and the exploration of a side gallery was accomplished with an operator guiding the mission. After the exploration maneuvers were performed, the pitch reference was set to $\theta = 1.5$ rad at $t \approx 4000$ s, to ascend the shaft in a nose-up configuration (see Fig. 6(d)). However, while resurfacing, the response of the depth controller was deteriorated by the drag of the tether (see Fig. 6(b)), as did the pitch measurements. Thus, as a safety measure, the VPS was set once again to a nose-front until the end of the dive.

The complete exploration mission had a duration of 1.77 hr. For the descent of the shaft, the depth control system achieved a RMSE of 0.2273 m, while the pitch controller a RMSE of 0.0872 rad. Similarly for the resurfacing of the UX-1, the depth controller achieved a RMSE of 0.4756 m and the pitch control a RMSE of 0.0932 rad. These results are in accordance with the results obtained in the tests performed considering only the pitch motions. Furthermore, the error accumulated by the depth controller while resurfacing was much higher than the descent, this can be explained by the unstable behavior observed in the depth control with a nose-up configuration. The results obtained with the coupled motion tests demonstrate that the VPS integrated in the UX-1 underwater vehicle is functional and validates the motion component as capable of performing a real mission in the operating environment intended for the UX-1 platform.

V. Conclusion

This paper presents the design, including the derivation of the dynamic model, and experimental validation of the variable pitch system for the underwater explorer robot UX-1. The VPS is composed of a suspended mass whose rotation allows to change the vehicle inclination. This actuator is crucial for the maneuverability of the robot in the challenging operating environment for which it has been designed.

The intention for the development of the UX-1 underwater vehicle is to explore mostly uncharted sections of underground flooded mines. The experimental results, concerning pitch motion tests, where only the VPS and the pitch controller are involved, and a combination of pitch and heave motion tests, demonstrate the effectiveness of the proposed variable pitch system. In particular, though a simple proportional controller has been adopted, the promising control error and settling time shown in the experiments confirm that the proposed solution is suitable for flooded mine exploration.

Due to the constricted space available inside the watertight hull of the UX-1 platform, the VPS rotation was limited to range of $\gamma \approx [-1.74, 1.74]$ rad. This motion constraint will be the focus of future studies, in order to further optimize the placement of the components in the interior of the hull. Moreover, more advanced pitch motion control laws will be integrated to the software architecture, based on model predictive and adaptive control strategies, to compare the performance achieved against the baseline metrics obtained in this work.

References

[1] B. E. Schmidt et.al, "Sub-Ice Marine and Planetary Ecosystems: First Results from Below the McMurdo Ice Shelf," Astrobiology Science Conference, Chicago, Illinois, USA, 15-19 June, 2015.

[2] K. Bergh, O.K. Hagen and E. Berglund, "Autonomous mapping with AUVs using relative terrain navigation," OCEANS 2017 Anchorage, Anchorage, AK, 2017.

[3] M. Gary, N. Fairfield, W.C. Stone, D. Wettergreen, G. A. Kantor and J. M. Sharp, "3D Mapping and Characterization of Sistema Zacatón from DEPTHX (DEep Phreatic THermal eXplorer)," in Proc. of KARST08: 11th Sinkhole Conference ASCE, Tallahassee, FL, USA, 22-24 Sep, 2008.

[4] L. Lopes, N. Zajzon, B. Bodo, S. Henley, G. Zibret, T. Dizdarevic, "UNEXMIN: developing an autonomous underwater explorer for flooded mines," Energy Procedia, Volume 125, Pages 41-49, 2017.

[5] Eriksen, Charles C and Osse, T James and Light, Russell D and Wen, Timothy and Lehman, Thomas W and Sabin, Peter L and Ballard, John W and Chiodi, Andrew M, "Seaglider: A long-range autonomous underwater vehicle for oceanographic research," IEEE Journal of oceanic Engineering, 2001.

[6] Jones, C and Webb, D and Glenn, S and Schofield, O and Kerfoot, J and Kohut, J and Roarty, H and Aragon, D and Haldeman, C and Haskin, T and others, "Slocum glider extending the endurance," The 16th International Symposium on Unmanned Untethered Submersible Technology (UUST09).

[7] Loc, Mai Ba and Choi, Hyeung-Sik and Kim, Jun-Young and Yoon, Jongsu, "Design and control of an AUV with weight balance," Oceans-Yeosu Conference, IEEE, 2012.

[8] Tran, Ngoc-Huy and Choi, Hyeung-Sik and Bae, Jae-Hyun and Oh, Ji-Youn and Cho, Jong-Rae, "Design, control, and implementation of a new AUV platform with a mass shifter mechanism," International journal of precision engineering and manufacturing, vol. 16, pp. 1599-1608, Springer, 2015.

[9] Kaznov, Viktor and Seeman, Mattias, "Outdoor navigation with a spherical amphibious robot," International Conference on Intelligent Robots and Systems, IEEE/RSJ 2010.

[10] Seeman, Mattias and Broxvall, Mathias and Saffiotti, Alessandro and Wide, Peter, "An autonomous spherical robot for security tasks," International Conference on Computational Intelligence for Homeland Security and Personal Safety, IEEE, 2006.

[11] Bruhn, Fredrik C and Kratz, Henrik and Warell, Johan and Lagerkvist, Claes-Ingvar and Kaznov, Viktor and Jones, Jack A and Stenmark, Lars, "A preliminary design for a spherical inflatable microrover for planetary exploration," Acta Astronautica, vol. 3, pp. 618-631, 2008.

[12] Rust, Ian C and Asada, H Harry, "The eyeball ROV: Design and control of a spherical underwater vehicle steered by an internal eccentric mass," IEEE International Conference on Robotics and Automation, 2011.

[13] S. Zavari, A. Heininen, J. Aaltonen, K. T. Koskinen, "Early stage design of a spherical underwater robotic vehicle," System Theory, Control and Computing (ICSTCC), 2016 20th International Conference, IEEE, 2016.

[14] R. A. Suarez Fernandez, D. Grande, A. Martins, L. Bascetta, S. Dominguez and C. Rossi, "Modeling and Control of Underwater Mine Explorer Robot UX-1," in IEEE Access, vol. 7, pp. 39432-39447, 2019.

[15] R. A. Suarez Fernandez, Z. Milosevic, S. Dominguez and C. Rossi, "Motion Control of Underwater Mine Explorer Robot UX-1: Field Trials," in IEEE Access, vol. 7, pp. 99782-99803, 2019.

[16] J. Villa et al., "Mechanical subsystems integration and structural analysis for the autonomous underwater explorer," 2018 IEEE/RSJ International Conference on Intelligent Robots and Systems (IROS), Madrid, 2018.

[17] P. Romero Bernal, "Mechanical design and analysis of an attitude control subsystem for pitch angle of an autonomous explorer submarine," Masters thesis, 2017.

[18] T. Fossen, Handbook of marine craft hydrodynamics and motion control, John Wiley & Sons, 2011.

[19] SNAME (1950). "The Society of Naval Architects and Marine Engineers. Nomenclature for Treating the Motion of a Submerged Body Through a Fluid." In: Technical and Research Bulletin No. 125.